# Human SWI/SNF Drives Sequence-Directed Repositioning of Nucleosomes on C-myc Promoter DNA Minicircles†

Hillel I. Sims, Jacqueline M. Lane,‡ Natalia P. Ulyanova,§ and Gavin R. Schnitzler*

*The Department of Biochemistry, Tufts University Sackler School of Graduate Biomedical Sciences, Boston, Massachusetts 02111*

*Received May 9, 2007; Revised Manuscript Received July 25, 2007*

ABSTRACT: The human SWI/SNF (hSWI/SNF) ATP-dependent chromatin remodeling complex is a tumor suppressor and essential transcriptional coregulator. SWI/SNF complexes have been shown to alter nucleosome positions, and this activity is likely to be important for their functions. However, previous studies have largely been unable to determine the extent to which DNA sequence might control nucleosome repositioning by SWI/SNF complexes. Here, we employ a minicircle remodeling approach to provide the first evidence that hSWI/SNF moves nucleosomes in a sequence dependent manner, away from nucleosome positioning sequences favored during nucleosome assembly. This repositioning is unaffected by the presence of DNA nicks, and can occur on closed-circular DNAs in the absence of topoisomerases. We observed directed nucleosome movement on minicircles derived from the human SWI/SNF-regulated c-myc promoter, which may contribute to the previously observed "disruption" of two promoter nucleosomes during c-myc activation in vivo. Our results suggest a model wherein hSWI/SNF-directed nucleosome movement away from default positioning sequences results in sequence-specific regulatory effects.

The precise localization of nucleosomes is one of the most important factors influencing transcription factor binding and gene regulation. ATP-dependent chromatin remodeling complexes are expected to act as transcriptional coregulators at least in part by altering nucleosome positions (*1*, *2*). However, very little is known about the influence of DNA sequence on nucleosome repositioning by these complexes. Human SWI/SNF (hSWI/SNF[1]) is an evolutionarily conserved multiprotein chromatin remodeling complex containing a core catalytic ATPase domain of either BRG1 or hBRM. It functions as a transcriptional coactivator or corepressor when recruited to promoters by over two dozen different activator and repressor proteins, including p53 and Rb as well as virtually all of the nuclear hormone receptors (*3*, *4*). Mammalian SWI/SNF function is necessary for embryonic development and for the differentiation of muscle, adipose, and blood cells (*3*, *5*, *6*). Mutations or decreased expression of several hSWI/SNF subunits have also been observed in many types of human cancers, and BRG1 mutant heterozygous mice are highly predisposed to cancer formation (*3*, *7*).

Human SWI/SNF activity is important for the transcriptional activation of many genes, including the proto-oncogene c-myc, which is transcriptionally upregulated in many forms of human cancer (*8*, *9*). Chromatin immunoprecipitation experiments in vivo have shown that hSWI/SNF is present on the active c-myc promoter in proliferating T cells, but not the inactive promoter in resting T cells (*10*). hSWI/SNF is required for $\beta$-catenin-dependent activation of c-myc (*11*), suggesting that it may play a role in colorectal cancer and melanoma in which c-myc upregulation frequently results from uncontrolled activation of $\beta$-catenin (*8*). hSWI/SNF is also a required coactivator for estrogen receptor $\alpha$ (*12*), suggesting that it plays a role in the estrogen-dependent upregulation of c-myc, which has been proposed to be essential for growth of hormone-dependent human breast cancer cells (*13*). Under some conditions, hSWI/SNF promotes cell cycle arrest, together with a corresponding decrease in c-myc transcription (*14*−*16*). While the repressive effect on c-myc is likely to be a secondary effect of arrest, it may indicate a potential role for hSWI/SNF in c-myc repression as well as activation. Importantly, c-myc transcription is associated with chromatin alterations that may result from hSWI/SNF action. Under conditions where c-myc was transcriptionally inactive, low-resolution mapping experiments indicated the presence of several positioned nucleosomes covering the c-myc promoter (*17*−*19*). Upon c-myc activation two of these nucleosomes situated over the P1 and P2 promoters (which are responsible for ∼90% of all c-myc gene transcription (*20*)) become "disrupted", meaning that MNase-accessible regions corresponding to

† This work was funded by grants to G.R.S. from the American Cancer Society (RSG-04-188) and the National Cancer Institute (K01CA88835).

* Address correspondence to this author. Tufts University School of Medicine, 136 Harrison Ave., Boston, MA 02111. Tel: (617) 636-2441. Fax: (617) 636-2409. E-mail: gavin.schnitzler@tufts.edu.

‡ Current address: Department of Nutrition and Genetics, Tufts University School of Nutrition and Science Policy, Boston, MA 02111.

§ Current address: Brigham & Women's Hospital, Division of Rheumatology, Immunology, and Allergy, Department of Medicine, Harvard Medical School Smith Building, One Jimmy Fund Way, Boston, MA 02115.

[1] Abbreviations: hSWI/SNF, human SWI/SNF; MNase, micrococcal nuclease; NPS, nucleosome positioning sequence; PAGE, polyacrylamide gel electrophoresis; EMSA, electrophoretic mobility shift analysis; SDS, sodium dodecyl sulfate; GGB, glycerol gradient buffer; ISWI, imitation switch; NURD, nucleosome remodeling deacetylase complex; $M_o$, minicircle octamers.

10.1021/bi7008823 CCC: $37.00 
Published on Web 09/18/2007

linker DNA between nucleosomes could no longer be readily detected by indirect end labeling. One potential explanation for this apparent disruption is that nucleosomes have been moved away from their initially favored positions by hSWI/SNF.

Our prior studies using atomic force microscopy on polynucleosomal DNAs clearly demonstrated nucleosome repositioning by hSWI/SNF (*21*). In addition, we also found that hSWI/SNF action on polynucleosomal templates resulted in stable changes in restriction enzyme accessibility, causing the most highly nucleosome-occluded sites to become the most accessible and vice versa (*21*, *22*). A similar effect was also seen for yeast SWI/SNF remodeling of a trinucleosomal template (*23*). While these studies hinted at a possible sequence-specificity in hSWI/SNF-dependent nucleosome repositioning, they provided only very low-resolution information about nucleosome positions. Furthermore, we have shown that hSWI/SNF forms abundant structurally altered dinucleosomes (altosomes) on polynucleosomal templates, which are characterized by an unusual nuclease accessibility profile (*22*). Thus, it was possible that altosome formation, rather than repositioning of normal nucleosomes, could have been responsible for the observed changes in restriction enzyme accessibility due to hSWI/SNF action. Attempts to provide more detailed information about how DNA sequence affects nucleosome repositioning by human and yeast SWI/SNF, in our lab as well as others, have employed short-length linear DNA sequences with one or two nucleosomes (*24*−*30*). Unfortunately, these studies encountered the problem that nucleosomes are generally repositioned by SWI/SNF to the ends or over the edges of linear DNA fragments, regardless of the sequence used.

Our current study avoids both of the problems associated with earlier studies (altosome formation as well end-positioning effects) by using mononucleosome minicircles to examine the specificity of hSWI/SNF-directed nucleosome repositioning in the absence of DNA ends. Such minicircle templates were previously employed to examine the relationship between DNA topology and nucleosome structure (*31*), but had not been used for remodeling experiments until now. The results from two c-myc promoter sequence mononucleosome minicircles, as well as a third 5S rDNA positioning sequence minicircle, indicate that hSWI/SNF moves mononucleosomes away from initially favored, nucleosome positioning sequences. These observations give new insights into the possible mechanisms by which human SWI/SNF regulates its target genes involved in cell growth, cell-cycle control, and cellular differentiation, as well as into general mechanisms of transcriptional control by chromatin remodeling complexes.

## EXPERIMENTAL PROCEDURES

*Creation of Minicircles.* C-myc promoter sequences were PCR amplified from human genomic DNA, ligated to CCGGAATTCCGG *Eco*RI linkers, and subcloned into pGEM 11 (Promega). Primers were P1_upper TGCGATGATTTATACTCACAGGACAAGGATGCGGT, P1_lower TCGGGGGTCCTCAGCCGTCCAGAC, P1/P2_upper TCGGCTGCCCGGCTGAGTCTCCTC and P1/P2_lower ATTACTACAGCGAGTTAGATAAAGCCCCGAAAACCGG. The *Xenopus borealis* 5S rDNA positioning sequence was PCR amplified from pXP10 (*32*), using the primers G G G G G A A G C T T G T G G A A T T G T G A G C G GATAACAATTTCACACAGG (upper) and AACCTTATGTATCATACACATAC (lower). The product was digested with *Hin*dIII, at sites internal to the top primer and 54 bp upstream of the bottom primer, and subcloned into pBluescript SK. To generate the template with *Apa*I ends, the 359 bp *Hin*dIII fragment was circularized using T4 DNA ligase, cut with *Apa*I and subcloned into pGEM 11. Minicircle sequences were PCR amplified and radiolabeled using primers flanking the plasmid polylinkers and a 1:20 ratio of $\alpha^{32}$P dATP to cold dATP. The products were digested with *Eco*RI or *Hin*dIII, separated by a 1% agarose gel, excised, and eluted by a QIAquick gel extraction kit (Qiagen).

*Minicircle Mononucleosome Assembly.* Nucleosomes were assembled onto the 359 bp linear DNA fragments by salt dilution using a 0.8:1 weight ratio of human HeLa cell core histones (*33*) to DNA, at room temperature, in 2 M NaCl, 10 mM Tris pH 7.5, 1 mM EDTA, 0.1 mg/mL BSA, 1 mM DTT, and 0.2 mM PMSF. Dilutions to 1.25, 0.9, 0.7, 0.6, 0.5, 0.4, and 0.3 M NaCl were done by adding the same buffer without salt every 10 min. Mononucleosomes were purified from dinucleosomes and bare DNA by ultracentrifugation on a 5% to 30% glycerol gradient, essentially as per Imbalzano et al. (*34*). Briefly, samples were layered onto a 5 mL linear gradient of glycerol gradient buffer (GGB) containing 50 mM Tris pH 7.5, 1 mM EDTA, 0.1 mg/mL BSA, 0.2 mM PMSF, and 5 to 30% glycerol, and samples centrifuged at 35,000 RPM for 16 h at 4 °C in a Beckman SW55 rotor. The gradient was fractionated into 200 $\mu$L aliquots, and peak mononucleosome fractions, identified by 4% polyacrylamide gel electrophoresis (PAGE) and autoradiography, were then exchanged into ligase buffer (NEB) by serial washes in a 10 kDa Millipore centrifugal filter. Ligation was performed at a DNA concentration below 0.3 ng/$\mu$L (which favors minicircle formation over intermolecular ligation (*31*)) using T4 DNA ligase at room temperature for 1 h. Ligated products were separated by 4% PAGE and the wet gel exposed to a Phosphorimager screen at 4 °C to identify all product locations. The $M_o$ form (mononucleosomal "minicircle octamer") was excised from the gel and eluted into 5% GGB overnight at 4 °C in the dark without shaking.

To form fully-closed-circular P1 minicircle mononucleosomes, the bare linear fragment was ligated in the presence of 0.3−0.45 $\mu$g/$\mu$L ethidium bromide, which favors formation of −1 supercoiled DNA minicircles (*31*). After electrophoresis and Phosphorimager analysis, the −1 supercoiled form was excised and eluted at 4 °C in TE overnight, followed by concentration using a 10 kDa Millipore centrifugal filter. Minicircle mononucleosomes were then assembled and purified as above. To measure the percentage of assembled minicircle mononucleosomes that were nicked, samples were treated with 0.2% SDS in order to remove histones, before resolution of topological forms by 4% PAGE. To correct for bare DNA circles that were present as a result of dissociation during $M_o$ purification, we subtracted the signal for the −1 supercoiled or nicked/−0 bare DNA forms that were present when the sample was separated by EMSA without SDS (e.g., Figure 1B) from the signal for that form after SDS treatment. The percentage of nicked minicircle mononucleosomes in the sample was then

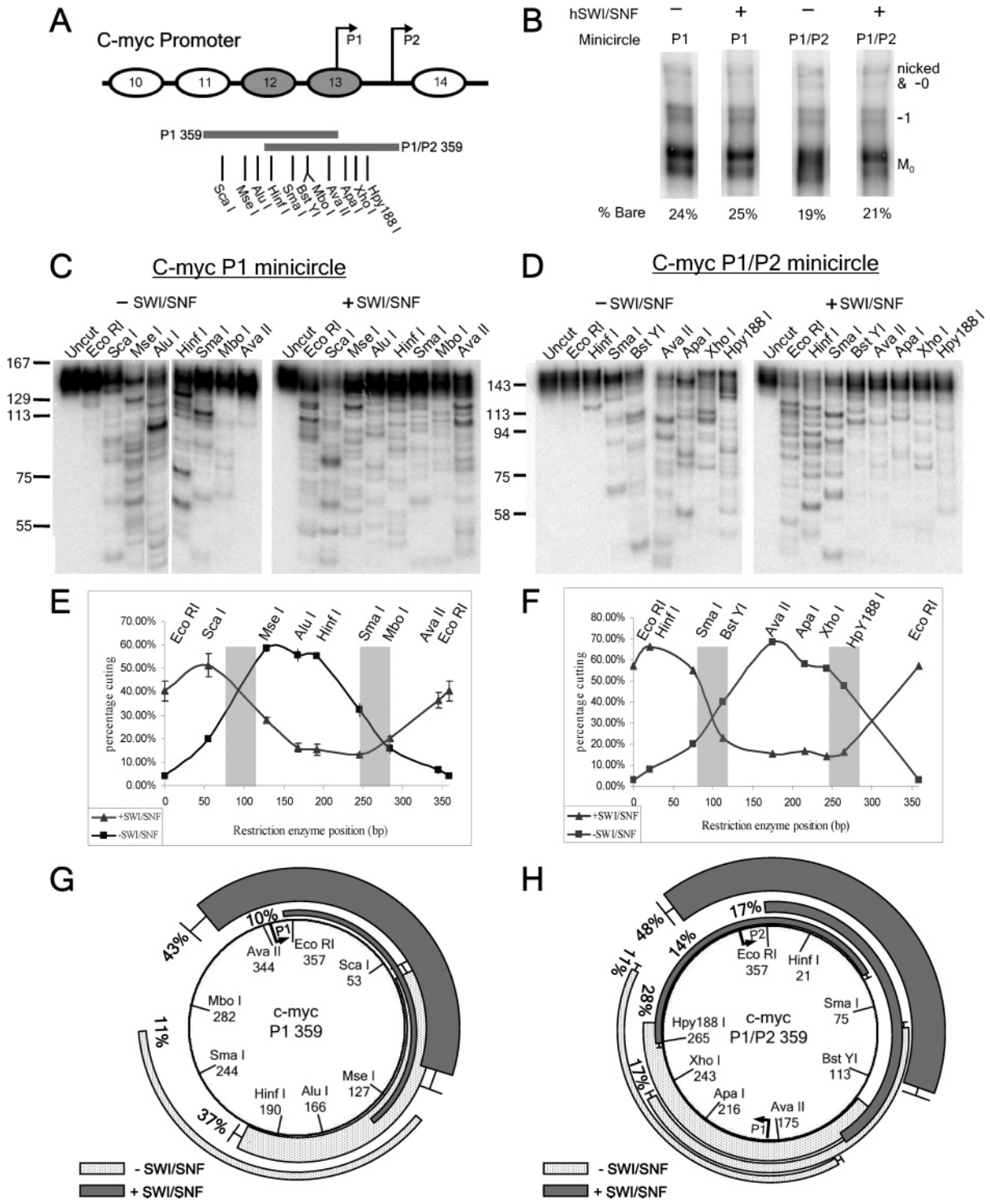


FIGURE 1: hSWI/SNF moves nucleosomes away from *c-myc* promoter positioning sequences. (A) *C-myc* promoter map based on in vivo mapping results (*17*−*19*). Shaded ovals represent the approximate positions of nucleosomes present on the repressed promoter that are disrupted upon *c-myc* activation. The P1 and P1/P2 minicircle sequences are represented by gray bars, with the locations of restriction sites indicated. (B) hSWI/SNF remodeling does not cause minicircle mononucleosome dissociation. Samples of hSWI/SNF-remodeled (+) and control (−) reactions on P1 and P1/P2 minicircles were treated with competitor DNA and polynucleosomes to eliminate hSWI/SNF binding (see Experimental Procedures), before 4% non-denaturing PAGE. The positions of the minicircle octamer ($M_0$) and bare DNA forms (−1 supercoiled and −0/nicked forms) are indicated on the right. The percentage of bare DNA was calculated as the signal due to bare DNA forms divided by the total amount of signal for the lane times 100%. Note that incubation in hSWI/SNF reaction buffer alone does not promote dissociation, since the percentage of bare DNA in the control reaction was the same as for a sample of the mononucleosome preparation immediately after gel isolation (data not shown). (C and D) Restriction enzyme digestion products for the 146 bp MNase fragments of the P1 and P1/P2 minicircle mononucleosomes with and without (+ or −) SWI/SNF remodeling. (E and F) Percent cutting graphs corresponding to the data in B and C. Shaded bars denote the approximate edges of *c-myc* nucleosomes 12 and 13 from the *in vivo* mapping studies. For B, the results show the average and standard error for two independent experiments. (G and H) Maps of each nucleosome position representing ≥10% of the P1 or P1/P2 minicircles. Light gray arcs: positions before hSWI/SNF treatment. Dark gray arcs: positions after hSWI/SNF remodeling. Bars at the ends of an arc indicate locations where overlapping nucleosome positions were within 10 bp of each other.

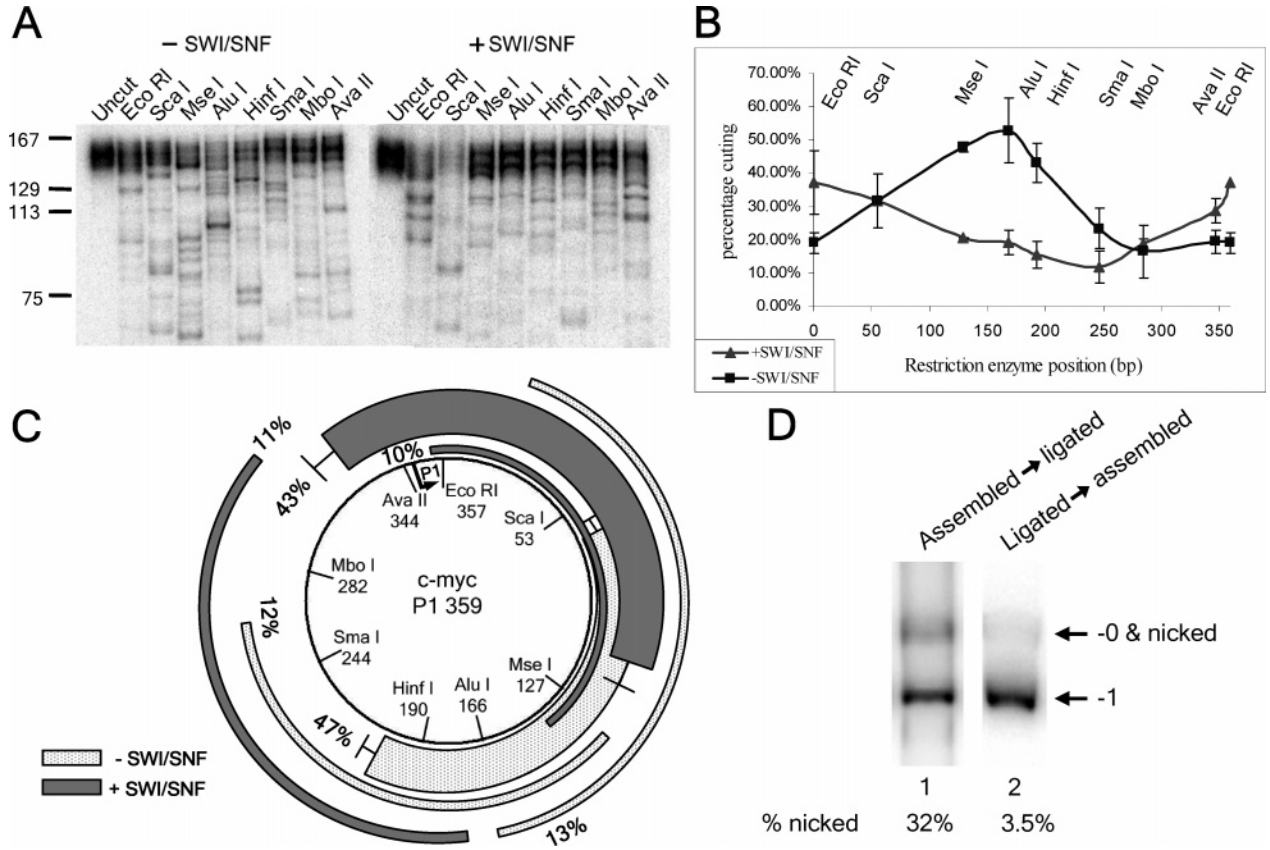


FIGURE 2: hSWI/SNF moves nucleosomes away from *c-myc* positioning sequences on fully closed-circular minicircles. Mapping results for control and remodeled fully closed circular −1 supercoiled P1 minicircles: (A) restriction digestion gels, (B) percentage cutting (showing the average values and standard error for two independent experiments), and (C) maps of major positions, as described for Figure 1. (D) Minicircle mononucleosomes derived from assembly onto the linear P1 template (lane 1) or circular P1 template (lane 2) were treated with SDS before PAGE, to measure the percentage of nicked and/or −0 closed circular DNA forms (which comigrate on the gel). Note that this DNA was associated with gel-isolated minicircle mononucleosomes. Given that the histone octamer constrains one negative supercoil, there should be virtually no mononucleosomal −0 closed circles. Thus, under the conditions used here, the percentage of nicked templates is expected to be almost equal to the percentage of templates that migrate as nicked/−0, after subtracting non-SDS treated control signal (see Experimental Procedures).

calculated by dividing the corrected signal for the −0/nicked forms by the total corrected signal for the −0/nicked and −1 forms and multiplying by 100%.

*SWI/SNF Remodeling and MNase Reactions.* hSWI/SNF was purified from HeLa cells by immunoaffinity chromatography against the FLAG-tagged Ini1 subunit (*35*). 25 ng of minicircle samples (∼1.1 nM) were reacted with 1.25 $\mu$g of hSWI/SNF (∼6.3 nM) in 100 $\mu$L reactions containing 0.4 $\mu$g/$\mu$L BSA, 65 mM KCl, 0.5 mM ATP, and 2.5 mM $MgCl_2$. For some reactions, wheat germ topoisomerase I (Promega) was added at a concentration of 0.1 units/$\mu$L. The reactions were incubated at 30 °C for 2.5 h, and hSWI/SNF remodeling was stopped by the addition of ADP to a concentration of 10 mM. Time course studies, using EMSA to resolve different nucleosome positions after hSWI/SNF remodeling (similar to Figures 3A and 3B), indicated that these remodeling conditions produce maximal changes in nucleosome positions after ∼10 min, with no further changes apparent after longer incubation (ref *24* and data not shown). These observations, together with the observation that remodeled positions are the same regardless of nucleosome starting positions (Figures 3 and 4), indicate that the remodeling conditions used here allow the repositioning reaction to reach an effective equilibrium, resulting in nucleosome positions that are most favored by hSWI/SNF. Note that, in preliminary studies on polynucleosomal templates, we see similar sequence-directed repositioning at a hSWI/SNF to nucleosome ratio of ∼1:9, arguing that the effects seen in these minicircle experiments are not an artifact of the higher hSWI/SNF:mononucleosome ratio used to ensure complete remodeling (H.I.S. and G.R.S., unpublished observations). For MNase digestion reactions: the buffer was adjusted to 1 mM $MgCl_2$, 3 mM $CaCl_2$, 60 mM KCl, 0.7 $\mu$g/$\mu$L BSA, 0.1 mM ATP, and 2 mM ADP in a total volume of 660 $\mu$L. The reactions were prewarmed for several minutes at 30 °C, digested with 0.2 unit/$\mu$L micrococcal nuclease (MNase, Roche unit definition) for 5 min, and stopped by adjusting the buffer to 0.2% SDS and 15 mM EDTA. MNase products were phenol extracted, ethanol precipitated in the presence of 50 $\mu$g of glycogen carrier, and separated by 4% PAGE. 146 ± ∼3 bp mononucleosomal products were then excised, eluted by continuous shaking at 37 °C in TE overnight, and concentrated using a 10 kDa Millipore centrifugal filter.

*Restriction Enzyme Digestion and Analysis of Nucleosome Positions.* Typically, for each restriction enzyme, >500 cpm of labeled ∼146 bp DNA was digested for 4 h in 20 $\mu$L reactions under supplier-specified ideal reaction conditions and using 10−20 units of each enzyme (enzymes were from New England Biolabs, with the exception of *Eco*RI, *Hinf*I, and *Eco*RV from InVitrogen and *Sma*I from Promega). The products were then separated by 8% PAGE along with a radiolabeled 100 bp NEB DNA ladder, and the gels were

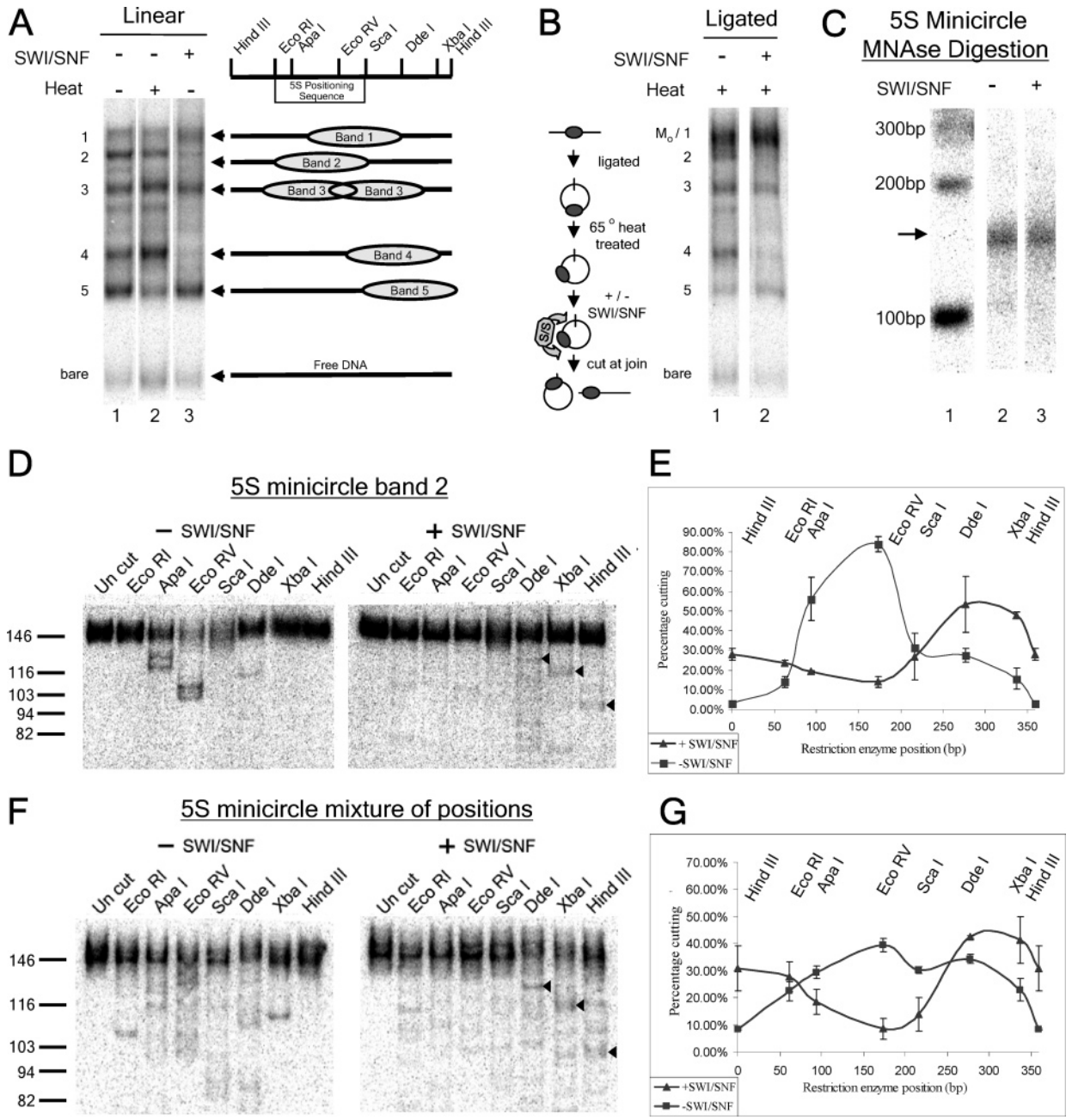


FIGURE 3: hSWI/SNF moves nucleosomes away from a 5S positioning sequence, and independent of starting position. (A) Mononucleosomes assembled onto the linear 359 bp *Xenopus borealis* 5S rDNA template with *Hin*dIII ends were purified by gradient ultracentrifugation. These were incubated in the absence of hSWI/SNF (lane 1), the presence of SWI/SNF and ATP (lane 3), or heated to 65 °C for 10 min, to promote movement to thermally favored positions (lane 2). Numbers on left: the five major gel shift positions/bands present after assembly. Cartoon on right: the nucleosome positions corresponding to each assembly-favored gel shift band, as determined by elution from the gel and MNase/restriction enzyme mapping (data not shown). (B) Ligated templates were heat treated, followed by incubation without hSWI/SNF (lane 1) or with hSWI/SNF (lane 2). hSWI/SNF activity was inhibited by addition of competitor DNA and chromatin, followed by *Hin*dIII digestion to release linear products. Cartoon on left: Experimental outline. $M_o$ indicates the position of the uncut minicircle mononucleosome ("minicircle octamer"), which comigrates with linear band 1. (C) 5S minicircle mononucleosomes ligated at the *Hin*dIII site were treated without hSWI/SNF (lane 2) or with hSWI/SNF (lane 3), followed by addition of ADP to stop remodeling before MNase digestion (see Experimental Procedures). MNase footprint products were resolved by 4% PAGE, and the wet gel exposed to a Phosphorimager screen for 30 min at 4 °C to identify ~146 bp mononucleosomal footprint products (arrow on left), which were subsequently excised from the gel and eluted. Lane 1: $^{32}$P end-labeled 100 bp ladder. (D−G) 359 bp *Xenopus borealis* 5S rDNA minicircles with (D) almost all histone octamers localized to the 5S positioning sequence (from ligation of band 2 mononucleosomes) or with (F) multiple octamer positions resulting from circularization of an even mixture of linear mononucleosomes isolated from bands 1 through 5 were treated with or without hSWI/SNF, and nucleosome positions mapped as described in Figure 1. Arrowheads highlight strong bands observed after hSWI/SNF remodeling on both minicircles. (E and G) Percent cutting plots showing the averages and standard errors for the results shown in D and F as well as a duplicate experiment. For (D), the signal was increased by kinase labeling MNase fragments with $\gamma^{32}$P-ATP before isolation of 146 bp products. Some DNA contaminants in the glycogen carrier were also labeled, giving rise to copurifying ~146 bp contaminant DNAs. We corrected for the percentage of signal due to these contaminants by subtracting the ~146 bp signal remaining after digestion of the MNase products with all seven restriction enzymes at once. The presence of this contamination did not obscure the underlying result, as indicated by the similarity between the experiment shown in (D) and a duplicate experiment where fragments were not kinase labeled (error bars in (E)).

dried. Reactions containing full-length 359 bp linear DNA fragment digested with the same enzymes were also included as a control for complete restriction enzyme cleavage. The dried gels were exposed to a Phosphorimager screen, and quantitated using ImageQuant software. To determine percent cutting, the signal for all restriction enzyme-digested products (bands smaller than the 146 bp MNase-digested input DNA) was divided by the total signal in the lane. To map individual nucleosome positions, band lengths were calculated by comparison to the ladder and/or digestion control lanes using FluorChem 8800 software. Restriction sites were chosen (spaced every ~50 bp apart) such that any nucleosome position must cover at least two sites, which allows nucleosome positions to be mapped by comparing bands from adjacent restriction sites. To determine the fraction of nucleosomes occupying each position, the signal from the larger of each pair of bands in a lane (>73 bp) was multiplied by 146 and divided by the length of the larger fragment. This calculation corrected for the intensity of the smaller band, simplifying the analysis and also accounting for fragments smaller than ~20 bp which were not resolved by the gel. The percentage of nucleosomes in any position was then calculated by dividing this corrected intensity by the signal for the entire lane and multiplying by 100%.

*Gel Shift Analysis of Nucleosome Positions Resulting from Assembly, hSWI/SNF, or Heat Treatment.* For linear 5S 359 bp mononucleosomes, standard remodeling reactions were incubated with or without hSWI/SNF for 1 h at 30 °C, or heated to 65 °C for 10 min (to promote movement to thermally favored positions). Remodeling was then stopped, and hSWI/SNF removed from the template, by addition of competitor DNA and chromatin (1 $\mu$g each of HeLa cell polynucleosomes and unrelated, supercoiled plasmid DNA). The different nucleosome positions were then resolved by 5% PAGE. To analyze minicircle mononucleosomes, 5S 359 bp linear mononucleosomes with *Hin*dIII ends were incubated with T4 DNA ligase in hSWI/SNF buffer for 1 h, followed by heat treatment at 65 °C for 10 min (to both inactivate the ligase and promote thermally favored nucleosome positions). The ligated template was then incubated at 30 °C for 1 h with or without hSWI/SNF, followed by addition of 1 $\mu$g each of competitor DNA and polynucleosomes to stop the remodeling reaction. Reactions were then digested with 10 units of *Hin*dIII at 30 °C for 1 h, followed by PAGE, to examine the nucleosome positions of the linear forms released by *Hin*dIII digestion. To determine the fraction of templates that remained circular, a sample of each reaction was treated with 2% SDS and proteinase K, followed by 5% PAGE to resolve circular and linear forms.

## RESULTS

Two 359 bp DNA fragments from the P1 and P2 region of the hSWI/SNF-regulated *c-myc* gene promoter were PCR amplified and radiolabeled using a 1:20 ratio of $\alpha^{32}$P dATP to cold dATP. These fragments were centered over the approximate *in vivo* locations of two promoter nucleosomes that were previously shown to be "disrupted" upon *c-myc* activation (nucleosome 12, P1 359, and nucleosome 13, P1/P2 359, in Figure 1A (*17*, *18*)). These linear fragments with *Eco*RI ends were assembled into nucleosomes by salt dilution, and the purified mononucleosomes were ligated to form minicircles (referred to as $M_o$, for "minicircle octamers"). The 359 bp length allows mononucleosome formation and also permits the DNA ends to bend back together and form a nonstrained circle of normal B form DNA (*31*). To map nucleosome positions, the purified mononucleosome minicircles were digested with MNase in order to produce mononucleosome-size 146 bp fragments. These fragments were purified by gel electrophoresis and then subjected to restriction enzyme digestion using enzymes with unique sites spaced ~50 bp apart throughout the DNA sequence.

The percentage of mononucleosome minicircles that had a nucleosome over any given restriction enzyme site can be determined by measuring the percentage of 146 bp MNase fragments that are cut by each restriction enzyme. For example, the 146 bp nucleosome fragments from the P1 minicircle, when digested with *Alu*I, produced one strong band and several weaker bands below 146 bp, which together represented 60% of the total DNA in the lane (Figure 1C, "−SWI/SNF"). Percent cutting for each restriction enzyme can be graphed to give a curve representing the proportion of minicircles in each reaction that had a nucleosome covering each site (Figures 1E and 1F, "−SWI/SNF"). Note that previous *in vivo* mapping studies provided information about the locations of linker regions to either side of *c-myc* promoter nucleosomes 12 and 13, at an estimated resolution of ±20 bp (shaded bars in Figures 1E and 1F (*17*, *18*)). The percent cutting values for the P1 and P1/P2 minicircles indicate that a high percentage of nucleosomes are assembled over approximately the same locations *in vitro*. This close correspondence between *in vivo* and *in vitro* nucleosome positions indicates that these sequences are functional nucleosome positioning sequences.

The specific locations of individual nucleosomes on the minicircles can be mapped to a resolution of ±5 bp by measuring restriction fragment lengths and intensities for adjacent restriction sites. For example, 37% of the nucleosomes formed on the P1 minicircle give rise to the intense bands in the *Alu*I lane at 104 bp and in the *Hin*fI lane at 135 bp (Figure 1C, "−SWI/SNF"). This and other major assembly positions of nucleosomes (≥10% of the total) are shown as light gray arcs in Figures 1G and 1H. Minor positions representing 5−10% of nucleosomes also localized to the same region of the DNA, but for simplicity are not shown in Figures 1G and 1H. In addition, while we could not reliably map bands representing less than 5% of the total, almost all of these weaker bands were found near the major bands. Well-characterized naturally occuring nucleosome positioning sequences (NPSes), such as the 5S rDNA NPS, tend to result in several assembly-favored positions clustered around a few most highly favored positions (*36*−*40*). Accordingly, our results are consistent with the presence of locally strong NPSes near the centers of the 359 bp *c-myc* P1 and P1/P2 promoter sequences.

*hSWI/SNF Moves Nucleosomes Away from Positioning Sequences on C-myc Minicircles.* Minicircle mononucleosomes were treated with hSWI/SNF and ATP under conditions that allow for the hSWI/SNF-driven repositioning reaction to reach effective equilibrium (see Experimental Procedures). Accordingly, these experiments do not measure the initial positions adopted after the first hSWI/SNF-driven movement event, but instead are designed to determine the DNA sequences at which hSWI/SNF intrinsically prefers to leave nucleosomes after complete remodeling. To eliminate

any effect of remodeling during the MNase digestion reaction, hSWI/SNF activity was then inhibited by using a 20-fold molar excess of ADP, which competitively inhibits SWI/SNF ATPase function (*22*, *34*, *41*). For control reactions, minicircles were treated under equivalent conditions except that hSWI/SNF was omitted, or ADP was added to prevent remodeling before addition of SWI/SNF.

Strikingly, for both the P1 and P1/P2 minicircles, the percent cutting analysis showed that nucleosomes were almost entirely moved from their original positions by hSWI/SNF, and now covered sites on the opposite side of the minicircle (Figures 1E and 1F "+SWI/SNF"). Fine-scale mapping indicated that hSWI/SNF remodeling results in movement of mononucleosomes to a few strong and several weak positions, which are all far removed from the assembly-preferred positions established by the Nuc 12 and Nuc 13 positioning sequences (Figures 1G and 1H, dark gray bars). In no case was an assembly-preferred position present after remodeling on more than 5% of the minicircles. These results suggest that nucleosome repositioning by hSWI/SNF is strongly influenced by DNA sequence, and that hSWI/SNF may preferentially relocate nucleosomes away from positioning sequences. Note that control experiments showed that this hSWI/SNF treatment did not increase the percentage of bare DNA minicircles, indicating that remodeling did not result in removal of histones from the template (Figure 1B).

*The Final Position of Nucleosomes on Minicircles Is Not a Favored Position for Nucleosome Assembly.* Ligation of the linear 359 bp fragment to form a minicircle could potentially generate a new nucleosome positioning sequence from the DNA on either side of the joint. If this was the case, then hSWI/SNF might simply be moving nucleosomes from the known positioning sequence to a stronger, newly formed positioning sequence. While the fortuitous formation of new positioning sequences on both c-myc DNA minicircles seemed unlikely, we wanted to formally rule out this possibility. To do so, fully-closed-circular bare DNA minicircles were created by ligating the P1 linear DNA in the presence of ethidium bromide, which intercalates into the DNA backbone resulting in negative supercoiling of the ligated product DNA. The −1 supercoiled form was purified by PAGE and assembled by salt dialysis, and the mononucleosome minicircle was isolated by elution from PAGE. When assembly-favored nucleosome positions on these minicircles were mapped, the major positions were very similar to those seen for the P1 minicircle mononucleosomes assembled before ligation, indicating that no strong positioning sequence was formed at the joint sequences (compare "−SWI/SNF" results for the P1 template in Figure 1 and Figure 2). Assembly onto the circle did allow some low-abundance nucleosome positions to form over and around the *Eco*RI site (e.g., 20% cutting in Figure 2B, "−SWI/SNF"). However, the great majority of nucleosomes were still observed to form at the same assembly-preferred positions observed for assembly onto the linear template in Figure 1. Accordingly, these results confirmed that hSWI/SNF was not simply moving nucleosomes to a higher-affinity positioning sequence that was fortuitously formed at the minicircle ligation site, instead it confirms that the preference for nucleosome movement is away from the high-affinity positioning sequence on the minicircle.

*The Presence or Location of a Nick on Minicircles Does Not Affect Nucleosome Repositioning by hSWI/SNF.* As a result of the inherent inefficiency of DNA ligase, when linear 359 bp templates were circularized after mononucleosome assembly, a single DNA nick at the ligation site was left on about one-third of the minicircles. This could be observed by SDS treatment, which removes histones from the DNA, followed by PAGE (Figure 2D, lane 1, 32% nicked). By contrast, assembly onto closed-circular bare DNA yielded mononucleosome minicircles that were only 3.5% nicked (Figure 2D, lane 2). Theoretically, the presence of a DNA nick might alter the positions favored after remodeling. For instance, a nick might block repositioning past it, resulting in nucleosomes stalled at specific positions to the left and right of the ligation site on nicked templates. To test whether this was the case, we compared the frequencies of individual nucleosome positions after remodeling on the 32% nicked (linear assembly) and 3.5% nicked (circular assembly) P1 templates (Figures 1G and 2C). We found that the hSWI/SNF-favored positions were very similar in both cases, with the most noticeable difference being a position representing 11% of the total in Figure 2C (leftmost dark gray bar) that was only 8% in the experiment shown in Figure 1 (and thus did not make the 10% cutoff to be displayed in Figure 1G). These results argue against any strong effects of a DNA nick on the final preferred locations of hSWI/SNF-remodeled nucleosomes. This is consistent with recent studies using nicked linear templates, which indicated that repositioning by hSWI/SNF and other remodeling complexes was not greatly effected by single DNA nicks (*27*, *30*, *42*, *43*).

*Repositioning of Nucleosomes on Minicircles by SWI/SNF Occurs Despite Topological Constraints.* On closed-circular templates, twisting of the DNA comes at an energetic cost that is inversely proportional to the length of the DNA circle (*44*). As a result, chromatin remodeling reactions that produce unconstrained supercoils can be inhibited unless a topoisomerase is included in the reaction to relax the torsional strain. Specifically, on circular multinucleosomal templates, topoisomerase action was shown to be important for the ability of yeast and human SWI/SNF to promote the altosome-associated loss of nucleosome-constrained supercoils (*22*, *23*, *41*), and for yeast SWI/SNF to transiently increase restriction enzyme accessibility to nucleosome-occluded sites during ongoing ATP-hydrolysis (*23*). Intriguingly, we found that the effects of hSWI/SNF on minicircle mononucleosome positions was identical in reactions lacking or containing wheat germ topoisomerase I (TopoI), which relaxes both unconstrained positive and negative supercoils (Figure 1 and data not shown). Even more strikingly, TopoI was not required for repositioning on a mononucleosome minicircle that was 97% closed circular (Figure 2 "+SWI/SNF"). Control experiments indicated that no topoisomerase activities were associated with our purified hSWI/SNF (data not shown). Thus, these results indicate that stable hSWI/SNF-driven nucleosome repositioning is possible on topologically constrained templates where generation of unconstrained supercoils has a high energetic cost. The apparent difference in toposomerase requirement between SWI/SNF-dependent repositioning (this work) and transient restriction enzyme accessibility (*23*) could potentially arise from differences in reaction conditions. For instance, it is possible that repositioning, like transient restriction enzyme acces-

sibility, is also slowed down in the absence of TopoI, but that this was not detected under the equilibrium remodeling conditions used in our studies. Alternatively, our results may indicate that transient restriction enzyme accessibility does not arise solely from ongoing nucleosome repositioning (which would create moments where restriction sites are in accessible linker DNA), but also from the creation of a transient SWI/SNF-remodeled nucleosomal species whose formation is inhibited by torsional strain and which is not required for repositioning.

*hSWI/SNF Demonstrates Directed Nucleosome Movement Away from the 5S rDNA Positioning Sequence.* Analysis of our *c-myc* minicircles indicated that hSWI/SNF may have an intrinsic preference to move nucleosomes away from positioning sequences. To further examine this positioning effect, we made use of the well-characterized positioning sequence from the somatic 5S rDNA of *Xenopus borealis* (*32*). We assembled mononucleosomes onto a 359 bp DNA fragment containing the 5S positioning sequence. Linear mononucleosomes with histone octamers at different positions were then separated by polyacrylamide gel electrophoresis (PAGE), in which fragments bearing a centrally located nucleosome migrate more slowly than fragments bearing a nucleosome at the end of the DNA (Figure 3A, lane 1 (*24*, *45*)). Each of the five major mononucleosomal gel-shift positions was excised, eluted, and mapped by MNase and restriction enzyme digestion (Figure 3A, cartoons on the right). The linear species with a nucleosome localized over the 5S positioning sequence (band 2 in Figure 3A (*32*)) was circularized, and the circular form was purified. These 5S minicircle mononucleosomes were then subjected to remodeling by hSWI/SNF. In the control reaction, 88% of these minicircles had nucleosomes in two overlapping positions covering the 5S positioning sequence and separated by ~10 bp (Figures 3D and 3E "−SWI/SNF"). After remodeling by hSWI/SNF, it was observed that the majority of nucleosomes had been moved to a new location away from the positioning sequence, and that the area containing the positioning sequence had become the least occupied region of the minicircle (Figures 3D and 3E, "+SWI/SNF"). Together with the previous *c-myc* minicircle data, these results suggest that hSWI/SNF has an intrinsic preference to move nucleosomes away from positioning sequences.

*hSWI/SNF Does Not Generate Structurally Altered Nucleosomes on Minicircles.* Previous studies from our lab showed that, on polynucleosomal templates, hSWI/SNF generates abundant "altosomes" consisting of structurally altered dinucleosomes with altered histone−DNA contacts and reduced nucleosome-constrained negative supercoiling (*22*). One of the advantages of the mononucleosome minicircle system is that altosomes cannot be formed from a single nucleosome. Indeed, the characteristic ~220 bp and ~80 bp altosomal MNase products were not observed upon MNase digestion of hSWI/SNF-remodeled mononucleosome minicircles (Figure 3C and data not shown). Thus, use of mononucleosome minicircles has allowed us to examine the effects of DNA sequence on hSWI/SNF-directed nucleosome repositioning, uncomplicated by other hSWI/SNF remodeling effects.

*hSWI/SNF-Favored Positions Differ from Thermally Favored Positions.* Several studies have indicated that nucleosome positions established by salt dialysis *in vitro* can accurately represent *in vivo* nucleosome positions. For instance, the sequence characteristics determined for high affinity nucleosomes generated by salt dialysis assembly onto yeast genomic, mouse genomic, or random sequence DNA are very similar to those for naturally occurring nucleosome positions from yeast and chicken genomic chromatin (see ref *46* for comparison of all these conditions). However, nucleosome positions established during salt-dialysis assembly can be altered by treatment at elevated temperatures (e.g., refs *24*, *25*, *45*, *47*−*50*), suggesting that mammalian body temperature might promote some level of nucleosome redistribution *in vivo*. Thermal repositioning is most rapid at high temperatures (up to 65 °C) and in the absence of divalent cations or linker histones (*45*, *48*, *51*, *52*). In general, thermal repositioning appears to result in redistribution between sites that are all at least moderately favored during nucleosome assembly (causing increases in some moderately favored positions and decreases in some strongly favored positions). Evidence also suggests that thermal repositioning may sometimes favor movement of the histone octamer toward DNA ends (*53*).

Given the above characteristics of thermal repositioning, we did not expect that hSWI/SNF favored positions on minicircles (which are always at locations seen at a very low frequency after assembly) would be the same as thermally favored positions. To test this directly, we used EMSA analysis to compare thermally favored and hSWI/SNF-favored positions on both linear and circular mononucleosome templates. While this approach does not give detailed information about individual nucleosome positions, it is an efficient way to compare the effects of each treatment on the overall distribution of nucleosomes. As shown in Figure 3A, lane 2, 65 °C heat treatment of linear 359 bp 5S mononucleosomes induces thermal repositioning, resulting in decreases in bands 1, 2, and 5 and increases in bands 4 and 3, relative to the unheated control sample in lane 1. hSWI/SNF remodeling of the linear template gave positions that differed from heat treatment, resulting in loss of bands 2 and 4, and accumulation of band 5 nucleosomes at the end of the template (Figure 3A, lane 3). Since DNA ends are known to alter the positions of hSWI/SNF products, and might also influence heat-treatment positions, we next compared the effects of these treatments on minicircle templates, in the absence of DNA ends. To do this, we performed a ligation and recutting experiment (as outlined in the cartoon in Figure 3B). Briefly, linear mononucleosomes were ligated to form circles. These minicircle mononucleosomes were heat treated at 65 °C to promote thermal repositioning to heat-favored sequences, as well as to inactivate the ligase. Next, these ligated templates were treated with ATP alone or ATP and hSWI/SNF. Remodeling was then stopped, and hSWI/SNF removed from the template, by addition of a vast excess of competitor chromatin and DNA (1 $\mu$g of each), followed by digestion with *Hin*dIII. On all templates where the histone octamer does not cover the *Hin*dIII site, this results in release of linear mononucleosomes, allowing relative nucleosome positions to be compared. For the reaction lacking hSWI/SNF (Figure 3B, lane 1) heat treatment followed by *Hin*dIII digestion released a pattern of bands similar to the heat-treated linear sample, with bands 3 and 4 being strongest. This indicates that the same positions are preferred by heat treatment on both the

linear and circular templates. To determine the percentage of templates where the mononucleosome blocked *Hin*dIII access, leaving the "$M_o$" circular form, a sample of the reaction was treated with SDS to remove histones, and circular and linear forms separated by PAGE (data not shown). This showed that 36% of the heat-treated, unremodeled templates remained circular, indicating that heat treatment also promoted movement of some octamers over the *Hin*dIII site. hSWI/SNF treatment of the ligated, heat-treated minicircles (Figure 3B, lane 2) resulted in a very different pattern, in which all bands except band 1/$M_o$ and band 5 were decreased (with the greatest decrease in the heat-favored band, band 4). The percentage of uncut templates was also increased to 52%. This increase in fast migrating band 5 (nucleosomes near the DNA edge) and nucleosomes over the *Hin*dIII site is consistent with the 5S minicircle mapping results shown in Figures 3D and 3E, "+SWI/SNF". Importantly, while some gel shift positions (e.g., band 3) were similar under both conditions, the overall pattern indicates that heat treatment and hSWI/SNF result in very different distributions of nucleosome positions on the 5S minicircle. These results indicate that hSWI/SNF does not move nucleosomes to low-energy binding sites preferred either by thermal repositioning or by salt dialysis assembly.

*The Final Positions of Nucleosomes on Minicircles Are Independent of the Nucleosome Starting Positions.* The mapping experiments in Figures 1 and 3D all started with the majority of the nucleosomes localized to a specific region of each template (the apparent nucleosome positioning sequences). We wanted to determine whether nucleosomes would move to the same hSWI/SNF-remodeled positions if they started at different initial positions. To test this, we combined equal amounts of linear 5S mononucleosomes isolated from each of the gel-shift bands 1 through 5, followed by ligation and minicircle isolation. This created an even mixture of nucleosome starting positions (Figure 3F and 3G "−SWI/SNF", note the roughly equal cutting of all sites except for the *Hin*dIII ligation site). When this mixture was treated with hSWI/SNF, we found that the nucleosome positions were very similar to those seen after remodeling the minicircle with a nucleosome localized over the 5S positioning sequence (compare Figures 3F and 3G to Figures 3D and 3E, "+SWI/SNF"). Similar results were also seen upon hSWI/SNF remodeling of minicircles formed from purified "band 4" 5S mononucleosomes, on which the histone octamer is shifted ~130 bp away from the 5S positioning sequence (Figure 3A and data not shown).

To explore this issue further, we cut the 5S minicircle with *Apa*I, subcloned this linear fragment, and used the resulting vector to prepare a 359 bp template with *Apa*I ends. Nucleosome assembly followed by ligation of this template resulted in mononucleosome minicircles that were identical in sequence, but 28% nicked at the *Apa*I site (95 bp from the normal *Hin*dIII ligation site, see cartoon in Figure 3A). Note that, since the 5S positioning sequence was not intact on the *Apa*I linear template, it was impossible for nucleosomes to be assembled over this preferred sequence. When this template was remodeled by hSWI/SNF, the restriction enzyme digestion pattern and percent cutting graphs were essentially identical to those seen for hSWI/SNF treatment of mononucleosome minicircles formed from the linear 5S template with *Hin*dIII ends, which was 33% nicked at the *Hin*dIII site (Figure 4). This further indicates, together with the results in Figure 2, that the presence and/or location of a single DNA nick does not greatly alter hSWI/SNF repositioning specificity. In addition, the combined results from Figures 3D−G and Figure 4 show that the same remodeled positions are observed regardless of nucleosome starting positions. This argues that the positions observed after remodeling do not represent initial repositioning events, for which remodeled positions might be expected to remain nearby starting positions. Instead, these results indicate that the observed repositioning of nucleosomes to DNA sequences away from assembly-favored positions represents a hSWI/SNF-favored equilibrium state, which is independent of nucleosome starting positions.

## DISCUSSION

The question of how DNA sequence directs nucleosome repositioning by SWI/SNF complexes has long remained unanswered, largely due to the strong tendency of SWI/SNF complexes to move histone octamers to the ends of linear DNA fragments. Our results on mononucleosome minicircles provide the first evidence for sequence-directed nucleosome movement by any SWI/SNF-family remodeling complex, and indicate that hSWI/SNF moves nucleosomes away from assembly-favored positions established by nucleosome positioning sequences. They also indicate that hSWI/SNF-preferred positions differ from thermally favored nucleosome positions. Together with previous studies showing that SWI/SNF action on polynucleosomes can stably increase restriction enzyme accessibility at sites normally covered by nucleosomes (*21*−*23*), our results suggest that nucleosome movement away from positioning sequences will be a general property of hSWI/SNF-remodeled chromatin.

We find that hSWI/SNF action on *c-myc* promoter minicircles directs nucleosome movement away from assembly-favored positions corresponding to the approximate locations of nucleosomes 12 and 13 from the repressed *c-myc* promoter *in vivo*. This suggests that sequence-driven nucleosome repositioning by hSWI/SNF contributes to the observed "disruption" of these two nucleosomes upon *c-myc* activation. The apparent "disruption" of these two nucleosomes might also arise from the conversion of the nucleosomes to an altered nucleosomal form or removal of nucleosomal histones from the DNA, activities that have also been demonstrated for human and yeast SWI/SNF complexes. However, of the different types of SWI/SNF remodeling activity, repositioning is likely to be one of the most important, since *in vitro* comparisons indicate that altered nucleosome formation and histone removal often affect a smaller fraction of nucleosomes or are slower than repositioning (*1*, *2*, *22*, *54*).

One favored model for nucleosome repositioning argues that the translocation of a remodeling complex ATPase domain across the DNA phosphate backbone gives rise to a DNA loop or bulge on the nucleosomal surface, whose movement to the other side of the histone octamer results in repositioning (*55*−*57*). Our results demonstrate that nucleosome repositioning can occur on a topologically closed minicircle in the absence of topoisomerase action. This suggests that the formation of the initial DNA loop may be able to proceed without significant DNA twisting. Alterna-

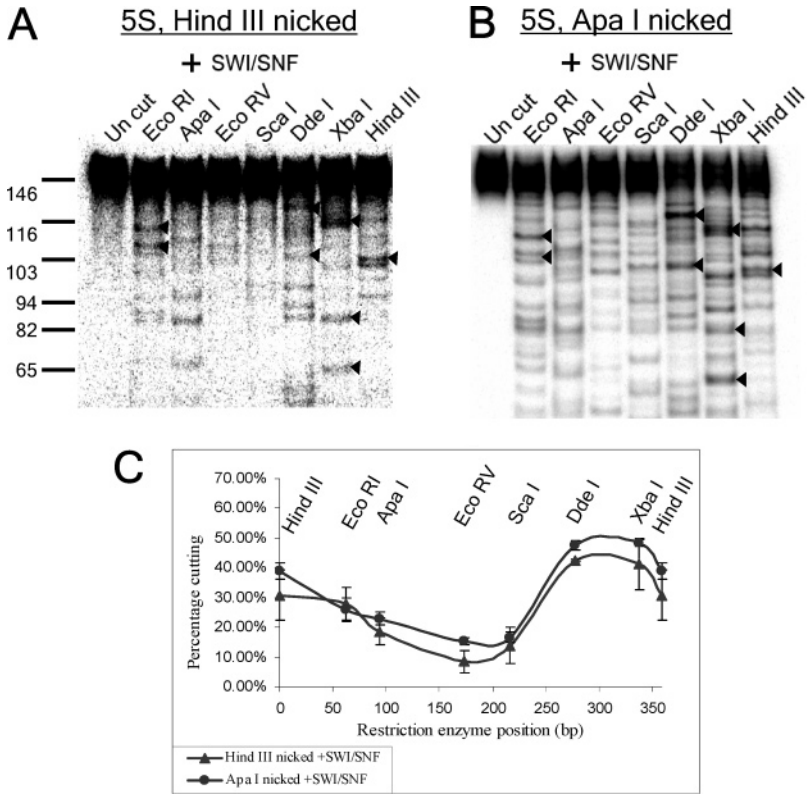


FIGURE 4: The distribution of remodeled nucleosomes is not altered by nucleosome starting position or the position of a DNA nick. (A) Restriction digestion pattern for hSWI/SNF-remodeled 5S minicircles, 33% nicked over the *Hin*dIII site of ligation. (B) Restriction digestion pattern hSWI/SNF-remodeled 5S minicircles formed by ligation of a 359 bp mononucleosome with *Apa*I ends, and, hence, 28% nicked over the *Apa*I site of ligation, 94 bp away from the *Hin*dIII site. Arrowheads indicate shared major bands. (C) Percentage cutting graphs showing the averages and standard errors for the results shown in A and B as well as one duplicate experiment.

tively, the energy afforded by ATP hydrolysis may be high enough to allow the formation of a supercoiled DNA loop, despite the high energetic cost of the unconstrained supercoils that would also be generated on these minicircle templates (*44*).

Two recent studies have indicated that ~50% of yeast nucleosome positions are specified by a nucleosome positioning sequence code, indicating that the control of nucleosome positions by DNA sequence is an unexpectedly common event (*46*, *58*). Our results suggest a model in which hSWI/SNF-activated gene promoters, such as *c-myc*, have been evolutionarily selected to encode nucleosome positioning sequences that place nucleosomes over important transcription factor binding sites. These nucleosome-occluded sites would then be opened up by hSWI/SNF-dependent repositioning away from these positioning sequences, when the complex is recruited to the promoter by transcriptional activators. Consistent with this model, we find that hSWI/SNF-directed nucleosome movement away from the nucleosome 13 positioning sequence uncovers the P1 promoter TATA box and initiation site (Figure 1H), which might directly promote *c-myc* transcription. The same model might also explain how hSWI/SNF can function as a corepressor when recruited to other target gene promoters (e.g., by Rb (*3*, *7*)): if default nucleosome positions facilitated the binding of transcriptional activators or blocked the binding of transcriptional repressors, then hSWI/SNF-directed repositioning away from these sequences would result in transcriptional repression. One recent study indicated that the yeast Isw2 remodeling complex repressed transcription by over-riding sequence-specified nucleosome positions that facilitated promoter accessibility (*59*). However, in contrast to our results, Isw2 remodeling did not appear to be affected by promoter DNA sequence, suggesting possible functional differences between ISWI and SWI/SNF class remodeling complexes. The idea that nucleosome positions can be functionally regulated by a combination of DNA sequence, SWI/SNF− and ISWI-class remodeling complexes, is also supported by a recent study showing that nucleosome positions on the yeast HIS3 gene differ considerably between wild-type, SWI/SNF- and ISW1- strains (*60*).

We find that certain mononucleosome positions are strongly favored after hSWI/SNF remodeling, and that these preferred locations are independent of nucleosome starting positions. This suggests that, in addition to directing movement away from positioning sequences, hSWI/SNF may have the additional property of placing mononucleosomes over specific hSWI/SNF-preferred sequences. It is unclear what makes a sequence a preferred location for hSWI/SNF-repositioned mononucleosomes. One hint comes from the observation that, in most cases, the positions to which hSWI/SNF moves nucleosomes are present at a low but measurable level after nucleosome assembly. For instance, in Figure 2A "+SWI/SNF" *Eco*RI lane, two preferred positions are represented by strong bands of ~129 and ~113 bp. These same bands are present, but at greatly reduced levels, in the "−SWI/SNF" control. These observations suggest that hSWI/SNF moves nucleosomes away from positions that are strongly preferred during assembly to positions that are unfavorable during assembly, but still allowed. Accordingly, hSWI/SNF appears not to move histone octamers to sequences that are incompatible with the assembly of a normal

nucleosome, but instead moves them to sequences that have some characteristics in common with nucleosome positioning sequences as well as some distinct, hSWI/SNF-preferred characteristics. It is hoped that ongoing studies comparing hSWI/SNF-favored positions on a variety of minicircle and polynucleosomal templates will provide further details about the nature of hSWI/SNF-favored sequences.

In summary, the use of mononucleosome DNA minicircles has provided an initial answer to the long-standing question of how DNA sequence directs nucleosome repositioning by hSWI/SNF. This work, however, is just a first step in understanding how repositioning by ATP-dependent remodeling complexes might affect DNA accessibility. Future application of the minicircle remodeling system developed here could provide insights into how transcription factor binding, variant core histones, linker histones, or histone tail modifications might alter the intrinsic sequence-specificity of hSWI/SNF-directed nucleosome positioning. In addition this system could be used to compare hSWI/SNF repositioning specificity to that of other remodeling complexes, such as those in the ISWI and NURD families, some of which may function by actively reversing hSWI/SNF remodeling effects. Finally, detailed studies on polynucleosomes will be necessary to determine where hSWI/SNF-altered dinucleosomal products (altosomes) are generated, and how repositioning specificity is influenced by the presence of neighboring nucleosomes.

## ACKNOWLEDGMENT

The authors would like to thank the National Cell Culture Center for FLAG-Ini1 HeLa cell culture, Brandi Davis and Kyle Havens for help with initial experiments, and Carol Kumamoto, Ananda Roy, Robert Kingston, and Geeta Narlikar for helpful comments on the manuscript.

## REFERENCES

1. Flaus, A., and Owen-Hughes, T. (2001) Mechanisms for ATP-dependent chromatin remodeling, *Curr. Opin. Genet. Dev. 11*, 148−154.
2. Ramachandran, A., and Schnitzler, G. (2004) Regulating transcription one nucleosome at a time: Nature and function of chromatin remodeling complex products, *Recent Res. Dev. Mol. Cell. Biol. 5*, 149−170.
3. Simone, C. (2005) SWI/SNF: The crossroads where extracellular signaling pathways meet chromatin, *J. Cell. Physiol. 207*, 309−314.
4. Chen, J., Kinyamu, H. K., and Archer, T. K. (2006) Changes in attitude, changes in latitude: nuclear receptors remodeling chromatin to regulate transcription, *Mol. Endocrinol. 20*, 1−13. Epub 2005 Jul 7.
5. Chi, T. (2004) A BAF-centred view of the immune system, *Nat. Rev. Immunol. 4*, 965−977.
6. Muller, C., and Leutz, A. (2001) Chromatin remodeling in development and differentiation, *Curr. Opin. Genet. Dev. 11*, 167−174.
7. Klochendler-Yeivin, A., Muchardt, C., and Yaniv, M. (2002) SWI/SNF chromatin remodeling and cancer, *Curr. Opin. Genet. Dev. 12*, 73−79.
8. Hermeking, H. (2003) The MYC oncogene as a cancer drug target, *Curr. Cancer Drug Targets 3*, 163−175.
9. Chung, H. J., and Levens, D. (2005) c-myc expression: keep the noise down!, *Mol. Cells 20*, 157−166.
10. Chi, T. H., Wan, M., Lee, P. P., Akashi, K., Metzger, D., Chambon, P., Wilson, C. B., and Crabtree, G. R. (2003) Sequential roles of Brg, the ATPase subunit of BAF chromatin remodeling complexes, in thymocyte development, *Immunity 19*, 169−182.
11. Barker, N., Hurlstone, A., Musisi, H., Miles, A., Bienz, M., and Clevers, H. (2001) The chromatin remodelling factor Brg-1 interacts with beta-catenin to promote target gene activation, *EMBO J. 20*, 4935−4943.
12. DiRenzo, J., Shang, Y., Phelan, M., Sif, S., Myers, M., Kingston, R., and Brown, M. (2000) BRG-1 is recruited to estrogen-responsive promoters and cooperates with factors involved in histone acetylation, *Mol. Cell. Biol. 20*, 7541−7549.
13. Doisneau-Sixou, S. F., Sergio, C. M., Carroll, J. S., Hui, R., Musgrove, E. A., and Sutherland, R. L. (2003) Estrogen and antiestrogen regulation of cell cycle progression in breast cancer cells, *Endocr. Relat. Cancer 10*, 179−186.
14. Hendricks, K. B., Shanahan, F., and Lees, E. (2004) Role for BRG1 in cell cycle control and tumor suppression, *Mol. Cell. Biol. 24*, 362−376.
15. Zhang, H. S., Gavin, M., Dahiya, A., Postigo, A. A., Ma, D., Luo, R. X., Harbour, J. W., and Dean, D. C. (2000) Exit from G1 and S phase of the cell cycle is regulated by repressor complexes containing HDAC-Rb-hSWI/SNF and Rb-hSWI/SNF, *Cell 101*, 79−89.
16. Nagl, N. G., Jr., Zweitzig, D. R., Thimmapaya, B., Beck, G. R., Jr., and Moran, E. (2006) The c-myc gene is a direct target of mammalian SWI/SNF-related complexes during differentiation-associated cell cycle arrest, *Cancer Res. 66*, 1289−1293.
17. Albert, T., Wells, J., Funk, J. O., Pullner, A., Raschke, E. E., Stelzer, G., Meisterernst, M., Farnham, P. J., and Eick, D. (2001) The chromatin structure of the dual c-myc promoter P1/P2 is regulated by separate elements, *J. Biol. Chem. 276*, 20482−20490.
18. Pullner, A., Mautner, J., Albert, T., and Eick, D. (1996) Nucleosomal structure of active and inactive c-myc genes, *J. Biol. Chem. 271*, 31452−31457.
19. Siebenlist, U., Hennighausen, L., Battey, J., and Leder, P. (1984) Chromatin structure and protein binding in the putative regulatory region of the c-myc gene in Burkitt lymphoma, *Cell 37*, 381−391.
20. Marcu, K. B., Bossone, S. A., and Patel, A. J. (1992) myc function and regulation, *Annu. Rev. Biochem. 61*, 809−860.
21. Schnitzler, G. R., Cheung, C. L., Hafner, J. H., Saurin, A. J., Kingston, R. E., and Lieber, C. M. (2001) Direct Imaging of Human SWI/SNF-Remodeled Mono- and Polynucleosomes by Atomic Force Microscopy Employing Carbon Nanotube Tips, *Mol. Cell. Biol. 21*, 8504−8511.
22. Ulyanova, N. P., and Schnitzler, G. R. (2005) Human SWI/SNF generates abundant, structurally altered dinucleosomes on polynucleosomal templates, *Mol. Cell. Biol. 25*, 11156−11170.
23. Gavin, I., Horn, P. J., and Peterson, C. L. (2001) SWI/SNF Chromatin Remodeling Requires Changes in DNA Topology, *Mol. Cell 7*, 97−104.
24. Ramachandran, A., Omar, M., Cheslock, P., and Schnitzler, G. R. (2003) Linker histone H1 modulates nucleosome remodeling by human SWI/SNF, *J. Biol. Chem. 278*, 48590−48601.
25. Flaus, A., and Owen-Hughes, T. (2003) Dynamic properties of nucleosomes during thermal and ATP-driven mobilization, *Mol. Cell. Biol. 23*, 7767−7779.
26. Fan, H. Y., He, X., Kingston, R. E., and Narlikar, G. J. (2003) Distinct strategies to make nucleosomal DNA accessible, *Mol. Cell 11*, 1311−1322.
27. Zofall, M., Persinger, J., Kassabov, S. R., and Bartholomew, B. (2006) Chromatin remodeling by ISW2 and SWI/SNF requires DNA translocation inside the nucleosome, *Nat. Struct. Mol. Biol. 13*, 339−346.
28. Kassabov, S. R., Zhang, B., Persinger, J., and Bartholomew, B. (2003) SWI/SNF Unwraps, Slides, and Rewraps the Nucleosome, *Mol. Cell 11*, 391−403.
29. Shundrovsky, A., Smith, C. L., Lis, J. T., Peterson, C. L., and Wang, M. D. (2006) Probing SWI/SNF remodeling of the nucleosome by unzipping single DNA molecules, *Nat. Struct. Mol. Biol. 13*, 549−554.
30. Aoyagi, S., and Hayes, J. J. (2002) hSWI/SNF-catalyzed nucleosome sliding does not occur solely via a twist-diffusion mechanism, *Mol. Cell. Biol. 22*, 7484−7490.
31. Prunell, A., Alilat, M., and Lucia, F. D. (1999) Nucleosome structure and dynamics. The DNA minicircle approach, *Methods Mol. Biol. 119*, 79−101.
32. Hayes, J. J., and Wolffe, A. P. (1992) Histones H2A/H2B inhibit the interaction of transcription factor IIIA with the *Xenopus borealis* somatic 5S RNA gene in a nucleosome, *Proc. Natl. Acad. Sci. U.S.A. 89*, 1229−1233.
33. Utley, R. T., Owen-Hughes, T. A., Juan, L. J., Cote, J., Adams, C. C., and Workman, J. L. (1996) In vitro analysis of transcription

factor binding to nucleosomes and nucleosome disruption/displacement, *Methods Enzymol. 274*, 276−291.
34. Imbalzano, A. N., Schnitzler, G. R., and Kingston, R. E. (1996) Nucleosome disruption by human SWI/SNF is maintained in the absence of continued ATP hydrolysis, *J. Biol. Chem. 271*, 20726−20733.
35. Schnitzler, G., Sif, S., and Kingston, R. E. (1998) Human SWI/SNF interconverts a nucleosome between its base state and a stable remodeled state, *Cell 94*, 17−27.
36. Becker, P. B. (2002) NEW EMBO MEMBER'S REVIEW: Nucleosome sliding: facts and fiction, *EMBO J. 21*, 4749−4753.
37. Buttinelli, M., Di Mauro, E., and Negri, R. (1993) Multiple nucleosome positioning with unique rotational setting for the Saccharomyces cerevisiae 5S rRNA gene in vitro and in vivo, *Proc. Natl. Acad. Sci. U.S.A. 90*, 9315−9319.
38. Fragoso, G., John, S., Roberts, M. S., and Hager, G. L. (1995) Nucleosome positioning on the MMTV LTR results from the frequency-biased occupancy of multiple frames, *Genes Dev. 9*, 1933−1947.
39. Tanaka, S., Livingstone-Zatchej, M., and Thoma, F. (1996) Chromatin structure of the yeast URA3 gene at high resolution provides insight into structure and positioning of nucleosomes in the chromosomal context, *J. Mol. Biol. 257*, 919−934.
40. Dong, F., Hansen, J. C., and van Holde, K. E. (1990) DNA and protein determinants of nucleosme positioning on sea urchin 5S rRNA gene sequences in vitro, *Proc. Natl Acad. Sci. U.S.A. 87*, 5724−5728.
41. Guyon, J. R., Narlikar, G. J., Sullivan, E. K., and Kingston, R. E. (2001) Stability of a Human SWI-SNF Remodeled Nucleosomal Array, *Mol. Cell. Biol. 21*, 1132−1144.
42. Langst, G., and Becker, P. B. (2001) ISWI induces nucleosome sliding on nicked DNA, *Mol. Cell 8*, 1085−1092.
43. Saha, A., Wittmeyer, J., and Cairns, B. R. (2002) Chromatin remodeling by RSC involves ATP-dependent DNA translocation, *Genes Dev. 16*, 2120−2134.
44. Clark, D. J., and Felsenfeld, G. (1991) Formation of nucleosomes on positively supercoiled DNA, *EMBO J. 10*, 387−395.
45. Meersseman, G., Pennings, S., and Bardbury, E. M. (1992) Mobile nucleosomes−a general behavior, *EMBO J. 11*, 2951−2959.
46. Segal, E., Fondufe-Mittendorf, Y., Chen, L., Thastrom, A., Field, Y., Moore, I. K., Wang, J.-P. Z., and Widom, J. (2006) A genomic code for nucleosome positioning, *Nature 442*, 772−778.
47. Pennings, S., Meersseman, G., and Bradbury, E. M. (1991) Mobility of positioned nucleosomes on 5 S rDNA, *J. Mol. Biol. 220*, 101−110.
48. Flaus, A., Rencurel, C., Ferreira, H., Wiechens, N., and Owen-Hughes, T. (2004) Sin mutations alter inherent nucleosome mobility, *EMBO J. 23*, 343−353.
49. Flaus, A., and Richmond, T. J. (1998) Positioning and stability of nucleosomes on MMTV 3′LTR sequences, *J. Mol. Biol. 275*, 427−441.
50. Kang, J. G., Hamiche, A., and Wu, C. (2002) GAL4 directs nucleosome sliding induced by NURF, *EMBO J. 21*, 1406−1413.
51. Ura, K., Hayes, J. J., and Wolffe, A. P. (1995) A positive role for nucleosome mobility in the transcriptional activity of chromatin templates: restriction by linker histones, *EMBO J. 14*, 3752−3765.
52. Sera, T., and Wolffe, A. P. (1998) Role of histone H1 as an architectural determinant of chromatin structure and as a specific repressor of transcription on Xenopus oocyte 5S rRNA genes, *Mol. Cell. Biol. 18*, 3668−3680.
53. Sakaue, T., Yoshikawa, K., Yoshimura, S. H., and Takeyasu, K. (2001) Histone Core Slips along DNA and Prefers Positioning at the Chain End, *Phys. Rev. Lett.* 87, 078105-1−078105-4.
54. Lorch, Y., Maier-Davis, B., and Kornberg, R. D. (2006) Chromatin remodeling by nucleosome disassembly in vitro, *Proc. Natl. Acad. Sci. U.S.A. 103*, 3090−3093.
55. Saha, A., Wittmeyer, J., and Cairns, B. R. (2005) Chromatin remodeling through directional DNA translocation from an internal nucleosomal site, *Nat. Struct. Mol. Biol. 12*, 747−755.
56. Flaus, A., and Owen-Hughes, T. (2003) Mechanisms for nucleosome mobilization, *Biopolymers 68*, 563−578.
57. Becker, P. B. (2005) Nucleosome remodelers on track, *Nat. Struct. Mol. Biol. 12*, 732−733.
58. Ioshikhes, I. P., Albert, I., Zanton, S. J., and Pugh, B. F. (2006) Nucleosome positions predicted through comparative genomics, *Nat. Genet. 38*, 1210−1215.
59. Whitehouse, I., and Tsukiyama, T. (2006) Antagonistic forces that position nucleosomes in vivo, *Nat. Struct. Mol. Biol. 13*, 633−640.
60. Kim, Y., McLaughlin, N., Lindstrom, K., Tsukiyama, T., and Clark, D. J. (2006) Activation of Saccharomyces cerevisiae HIS3 results in Gcn4p-dependent, SWI/SNF-dependent mobilization of nucleosomes over the entire gene, *Mol. Cell. Biol. 26*, 8607−8622.

BI7008823